Flinders UNIVERSITY

DOI: 10.1002/cnma.201400005

Application of Polymer Interlayers in Silicon-Carbon Nanotube Heterojunction Solar Cells

Leping Yu, Daniel D. Tune, Cameron J. Shearer and Joseph G. Shapter*[a]

Abstract: We explore the use of polymers as a conducting interlayer within silicon-carbon nanotube heterojunction photovoltaics. Three types of devices have been fabricated and characterized including silicon-carbon nanotube, silicon-conducting polymer and silicon-conducting polymer-carbon nanotube. The conducting polymers studied were polyaniline, poly(3-hexylthiophene-2,5-diyl) and poly(3,4-ethylenedioxythiophene): poly(styrene sulfonate). A thin conducting polymer interlayer significantly improves photovoltaic performance by creating a better depletion layer within the underlying silicon. With the addition of a top antireflection layer, a photovoltaic device, silicon-poly(3,4-ethylenedioxythiophene): poly(styrene sulfonate)-carbon nanotube-poly(styrene) has been fabricated with a photovoltaic conversion efficiency of 8.7 %.

Introduction

In order to overcome some of the production costs of conventional silicon-based solar cells, as well as to counter the toxicity and/or scarcity of some alternatives including indium, cadmium, ruthenium and lead, researchers have made great efforts in the last a few decades to pioneer the use of carbon materials as components of light harvesting devices [1]. One such material is carbon nanotubes (CNTs) which have shown excellent electronic and optical properties since their discovery in 1991 [2]. Si-CNT heterojunction solar cells are an alternative to conventional silicon devices, where the cost-intensive fabrication of a p-type silicon layer is replaced by deposition of a highly transparent CNT film [3]. The transparent film allows many incident photons to reach the silicon and be absorbed to create electron-hole pairs. Following exciton diffusion to the depletion region, created by the interaction of the p-type nanotubes and n-type silicon, dissociation occurs under the influence of the built-in potential resulting from equilibration of the silicon and CNT Fermi levels, with the holes and electrons acting as the majority charge carriers in the CNT and silicon layers, respectively [3e].
Polymers form another class of carbon-based materials which have also been studied as materials for solar cells using simple fabrication process [4]. So far, major efforts have been made in both Si-CNT and Si-organic solar cells separately [5]. For example, with the introduction of titanium dioxide as an antireflection layer, and following doping of the CNT film with HNO_3 and H_2O_2, a Si-CNT device with an efficiency of 15 % has been fabricated [6]. By using a broader range of the solar spectrum and by minimizing thermalization losses, a polymer solar cell with a tandem structure and efficiency of about 10 % has also been prepared [7]. Recently, researchers have started to apply polymers as antireflection layers and conducting interlayers in Si-CNT systems. Both polymethylmethacrylate (PMMA) and polydimethylsiloxane (PDMS) have been used as an antireflection top layer to help the silicon substrates absorb more energy from the incident light and the efficiencies of the resulting devices are above 10 % [3g, 8]. PDMS is also able to protect the silicon surface from air oxidation and the performance of such cells has been shown to be relatively stable for at least 20 days [3g]. Polyaniline (PANI) has been combined with silicon to form the heterojunction in the application of solar cells with very limited performance due to the low conductivity (below 10^{-1} S cm^{-1}) of the PANI film which is caused by the poor lateral current carrying capacity (ampacity) of the polymer film [9]. A poly(3,4-ethylenedioxythiophene): poly(styrene sulfonate) (PEDOT:PSS) thin layer has also been applied to planar silicon to form a heterojunction but performance is poor [10]. The performance can be improved by adding a MoO_3 antireflection layer [5b]. The poor lateral ampacity of PANI and Si-PEDOT:PSS layers can be improved by adding a metal grid[10a, 11], but the material such as silver is expensive which somewhat defects the purpose of using the polymer. When PANI acts as a conducting polymer interlayer between the silicon substrate and the CNT film, it has been shown to improve the performance of Si-CNT devices with the improvement explained in terms of a better depletion region which helps to separate the excitons more effectively in the silicon near the heterojunction interface [12]. Here, we systematically explore the use of selected conducting polymers (CPs) as interlayers between the silicon substrate and CNT film. Specifically, three polymers have been used; PANI, poly(3-hexylthiophene-2,5-diyl) (P3HT) and PEDOT:PSS. Three types of device have been prepared; Si-CNT, Si-CP, and Si-CP-CNT, as shown in Figure 1. Additionally, polystyrene (PS) was introduced as an antireflection top layer and a device with Si-PEDOT:PSS-CNT-PS structure was prepared.

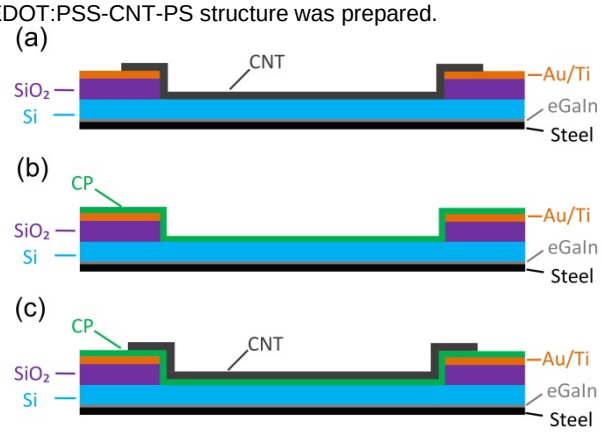

Figure 1. Schematic structures of (a) Si-CNT, (b) Si-CP and (c) Si-CP-CNT.

[a] Professor Joseph G. Shapter
Centre for Nanoscale Science and Technology
Flinders University
Bedford Park, South Australia 5042
E-mail: Joe.Shapter@flinders.edu.au

Supporting information for this article is given via a link at the end of the document.

Results and Discussion

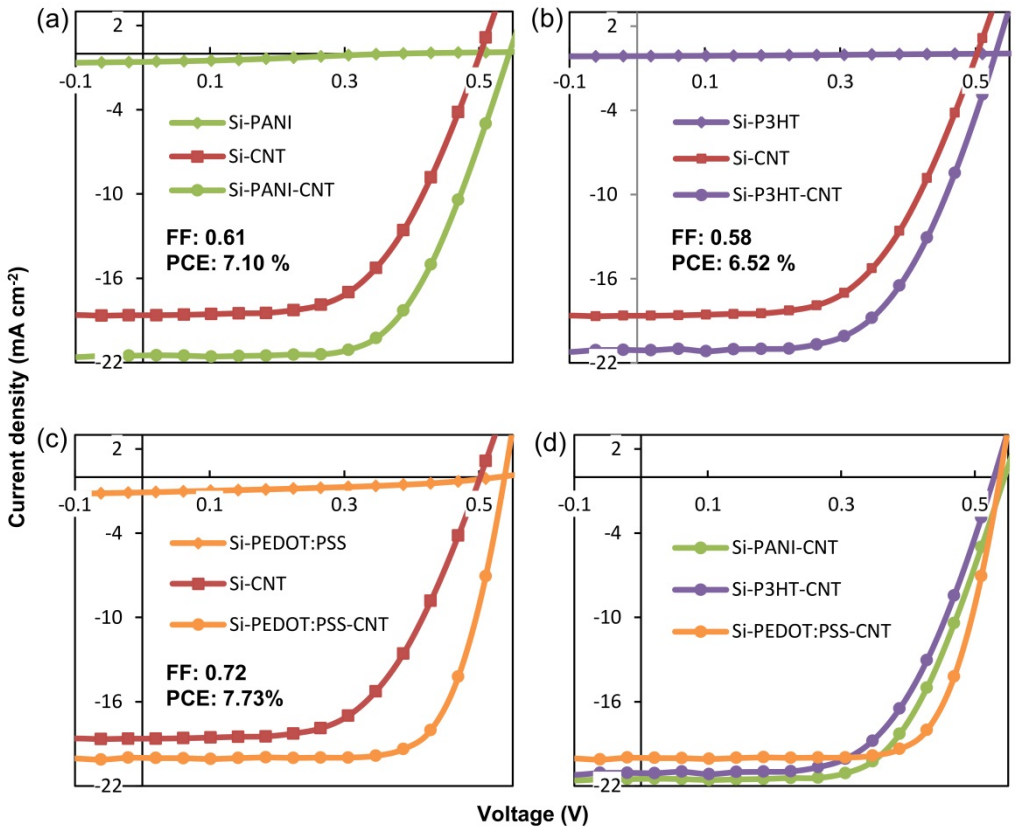

Figure 2. Current density-voltage measurements of solar cells with (a) PANI, (b) P3HT and (c) PEDOT:PSS. Each plot shows the light curves obtained from Si-CP, Si-CNT and Si-CP-CNT devices and (d) shows a comparison between Si-PANI-CNT, Si-P3HT-CNT and Si-PEDOT:PSS-CNT.

Figure 2 shows the current density-voltage (J-V) curves measurements of devices involving conducting polymer interlayers (EQE curves are shown in Figure S1). The polymer-only devices have very poor performance in all respects, including low short circuit current density (J_{sc}), open circuit voltage (V_{oc}), fill factor (FF), and power conversion efficiency (PCE) along with high ideality and reverse saturation current density (J_{sat}) (as detailed in Table 1). This is because the thin conducting polymer layer has limited ampacity, especially P3HT. Si-CNT devices show much better performance (Figure S2) compared to Si-CP devices because the CNT film has a lower sheet resistance ($R_{sheet} \approx 400\ \Omega$ square^{-1}) and higher ampacity than the conducting polymer layers ($R_{sheet} > 10^6\ \Omega$ square^{-1}). The PCE of the Si-CNT control device is normally around 5 % [3l]. After addition of PANI, P3HT or PEDOT:PSS between the silicon substrate and the CNT films, both J_{sc} and V_{oc} are improved compared to devices without the polymer (Table 1). Additionally, there is a significant increase in FF, especially after adding the PEDOT:PSS interlayer. The conducting polymer modified devices also have better ideality and 1-2 orders of magnitude lower J_{sat} compared to the devices without the polymer. These improvements indicate that a better depletion

Table 1. Average values (3 devices for each kind) of Si-CNT, Si-PANI, Si-PANI-CNT, Si-P3HT, Si-P3HT-CNT, Si-PEDOT:PSS-CNT. Parameters of the best cell in each group are in bold.

	J_{sc} (mA cm^{-2})	V_{oc} (V)	FF	PCE (%)	Ideality	J_{sat} (mA cm^{-2})
Si-CNT	**18.9** 18.5 ± 0.7	**0.51** 0.51 ± 0.02	**0.62** 0.61 ± 0.07	**6.00** 5.80 ± 0.53	**1.45** 1.50 ± 0.16	**1.43×10^{-5}** $2.42 \times 10^{-5} \pm 2.14 \times 10^{-5}$
Si-PANI	**0.6** 0.6 ± 0.1	**0.38** 0.37 ± 0.02	**0.3** 0.29 ± 0.04	**0.07** 0.07 ± 0.00	**4.46** 4.59 ± 0.19	**3.86×10^{-3}** $5.19 \times 10^{-3} \pm 1.53 \times 10^{-3}$
Si-PANI-CNT	**21.5** 1.3 ± 0.2	**0.55** 0.54 ± 0.01	**0.61** 0.61 ± 0.01	**7.10** 7.03 ± 0.08	**1.22** 1.27 ± 0.07	**3.16×10^{-4}** $4.83 \times 10^{-7} \pm 2.08 \times 10^{-7}$
Si-P3HT	**0.1** 0.1 ± 0.0	**0.40** 0.40 ± 0.02	**0.32** 0.32 ± 0.02	**0.02** 0.02 ± 0.01	**4.00** 4.00 ± 0.17	**2.61×10^{-4}** $2.61 \times 10^{-4} \pm 1.80 \times 10^{-4}$
Si-P3HT-CNT	**21.1** 20.8 ± 0.3	**0.53** 0.53 ± 0.01	**0.58** 0.59 ± 0.05	**6.52** 6.49 ± 0.23	**1.30** 1.34 ± 0.04	**1.36×10^{-6}** $5.69 \times 10^{-6} \pm 4.04 \times 10^{-6}$
Si-PEDOT:PSS	**1.1** 1.0 ± 0.2	**0.53** 0.52 ± 0.01	**0.38** 0.36 ± 0.02	**0.22** 0.19 ± 0.03	**2.22** 2.42 ± 0.19	**2.26×10^{-7}** $7.26 \times 10^{-5} \pm 5.00 \times 10^{-5}$
Si-PEDOT:PSS-CNT	**20** 20.0 ± 0.4	**0.54** 0.54 ± 0.01	**0.72** 0.69 ± 0.03	**7.73** 7.38 ± 0.31	**1.27** 1.30 ± 0.03	**6.87×10^{-7}** $8.90 \times 10^{-7} \pm 1.77 \times 10^{-7}$

region is formed in the silicon, meaning that electron-hole pairs can be separated more effectively. This is likely a result of the PANI, P3HT and PEDOT:PSS layers forming a conformal covering on the silicon surface whereas sparse CNT networks limit the overall photoactive junction interfacial area due to a smaller area with intimate contact between the p-type and n-type material [12a]. After introducing a conducting polymer interlayer between silicon and CNT film, there is a larger intimate contact area on silicon compared to CNT film. Thus, the ability to collect charge carriers in the Si-CNT device is worse than that of Si-PANI-CNT, Si-P3HT-CNT and Si-PEDOT:PSS-CNT cells. As shown in Figure 2 (d), all three conducting polymer modified Si-CNT solar cells have similar V_{oc} with slight differences in J_{sc}. However, the FF of the Si-PEDOT:PSS-CNT device is 0.11 - 0.14 higher than that of the other two devices. For this reason, the Si-PEDOT:PSS-CNT has the highest PCE (7.7 %) among the three.

As shown in Figure 3, the surfaces of all 3 polymer interlayers are not smooth and therefore it is difficult to assess the thickness of these layers accurately. The surface of the P3HT is the roughest (root-mean-square: 4.21 nm), while the surface of PEDOT:PSS is the smoothest (root-mean-square: 1.85 nm), as shown in Figure S3. This feature might have an impact on the performance of devices. The smoothest layer (PEDOT:PSS) leads to less light scattering while rougher layers scatter more light. The thickness of each of the 3 polymer layers is less than approximately 10 nm, which is thin enough not to hamper the transport of charge carriers to the CNT films.

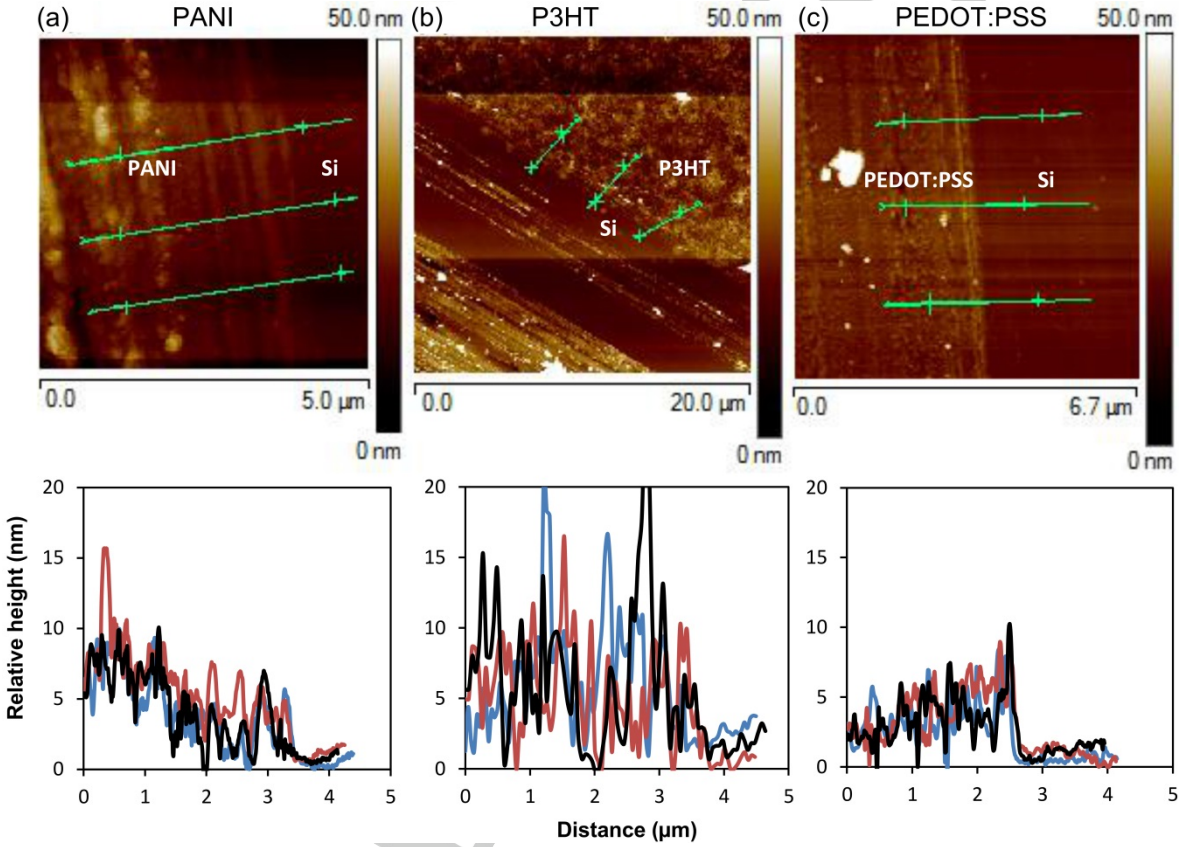

Figure 3. AFM height images of (a) PANI, (b) P3HT and (c) PEDOT:PSS films on silicon. Lines on the images correspond to the relative height traces used to measure the film thickness in the lower plots.

Figure 4 shows the change in performance of the solar cells when made using different PANI layer thicknesses, which is directly related to the number of PANI drops spin-coated onto the silicon surface. The '0 drop' device represents the Si-CNT device without any polymer, with a PCE of 5.3 % (see Figure S2). After the introduction of a 3 drop PANI interlayer, the performance of devices improved to 7.1 %. For the devices with thicker PANI films (5 drops), the performance starts to decrease, likely due to less efficient transport of holes from silicon to the CNT film, which increases recombination of the separated charge carriers. For the devices with very thick PANI layers (10-15 drop devices), the transport of holes to CNT films is blocked completely because the polymer layers are not doped entirely during the fabrication. As a result, these devices have very poor performance, with PCE < 0.1 %. Thus it is clear that the improved performance of the cells with the conducting polymer interlayers depends on having the optimal layer thickness.

Given that the PEDOT:PSS cells gave the best performance, further efforts to improve this performance were undertaken. As discussed earlier, adding an antireflection layer such as PDMS or PMMA has been shown to increase the performance of Si-CNT devices by helping the silicon surface to trap more energy from the incident light [3g, 8]. Here, another polymer material, PS,

has been used for the same purpose to build Si-PEDOT:PSS-CNT-PS cell. The influence of a series of treatments applied to the devices post-fabrication (but before PS addition) is shown in Figure 5, and Table 2 summarizes the important parameters of a typical cell. The as-prepared, untreated device has limited performance as was the case for the Si-CNT devices, including a high series resistance and low shunt resistance, J_{sc}, FF and PCE. Compared to the Si-CNT cells shown in Figure S2 (a), the

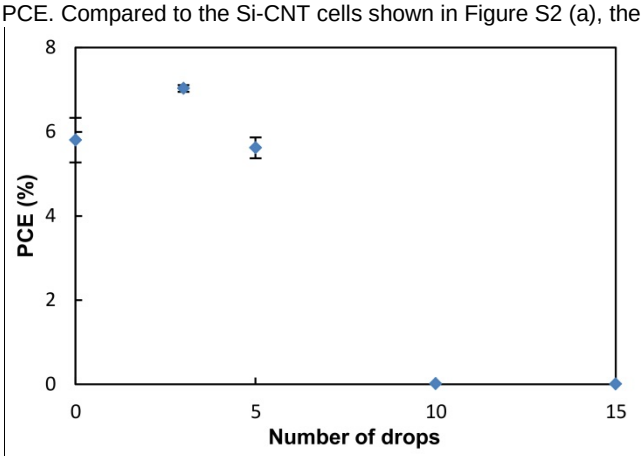

Figure 4. The influence of the number of PANI drops (0, 3, 5, 10 and 15) spin-coated onto the silicon surface on the PCE of Si-PANI-CNT devices. 0 drops represents the performance of Si-CNT. The J-V light curve of the 3-drop device was shown in Figure 2 (a) and the J-V light curves of 0-drop and 5/10/15-drop devices can be found in Figure S2.

performance is improved considerably after hydrofluoric acid (HF) treatment. This could be due to the fact that HF has a light doping effect via protonation of the PEDOT in the PEDOT:PSS interlayer. As a result, the ability to maintain separation of electron-hole pairs has been improved and the cell has a higher FF (0.46) compared to that of a similarly treated Si-CNT device (0.27, as shown in Figure S2). However, after $SOCl_2$ treatment the performance decreases in the same manner as for Si-CNT devices. After a second HF treatment, the performance of the Si-PEDOT:PSS-CNT device is improved again due to a slight increase of J_{sc}, V_{oc} and a dramatic increase of the FF, from 0.28 to 0.72. As shown in Figure 5 and Table 2, after adding the PS antireflection layer there is a clear improvement of J_{sc} and the PCE is increased to 8.7 % due to increased incident light absorption by the silicon because of the reduced reflectance of the surface. Reflectance curves are provided in Figure S4.

Table 2. Parameters obtained from J-V light curves of the 4-layer structure (Si-PEDOT:PSS-CNT-PS) after each successive fabrication step.

	As prepared	1st HF	$SOCl_2$	2nd HF	PS
J_{sc} (mA cm^{-2})	1.2	19.8	19.2	20.0	24.5
V_{oc} (V)	0.52	0.49	0.48	0.54	0.54
FF	0.19	0.46	0.28	0.72	0.66
PCE (%)	0.12	4.43	2.61	7.73	8.66
R_{shunt} (Ohm)	3.57×10^3	5.63×10^3	2.47×10^3	2.38×10^3	7.50×10^3
R_{series} (Ohm)	2.29×10^4	2.07×10^2	7.77×10^2	4.77×10^1	5.07×10^1

Figure 6 shows the relative degradation of Si-CNT solar cells with different conducting polymer interlayers, and with a PS antireflection layer. The main symptom of the degradation is the decrease in FF. The Si-CNT cell has the fastest initial degradation rate, probably because the CNT network on the surface is sparse, which leads to large exposed areas of silicon reacting with oxygen in air. Compared to Si-CNT devices, the degradation rate of Si-PANI-CNT, Si-P3HT-CNT and Si-PEDOT:PSS-CNT is slightly slower for the first 2 days. After 7 days, the PCE of Si-PANI-CNT cell is the lowest, which could be due to a slow deprotonation process in the PANI layer, which then accelerates the oxidation of the silicon. The fact that V_{oc} of

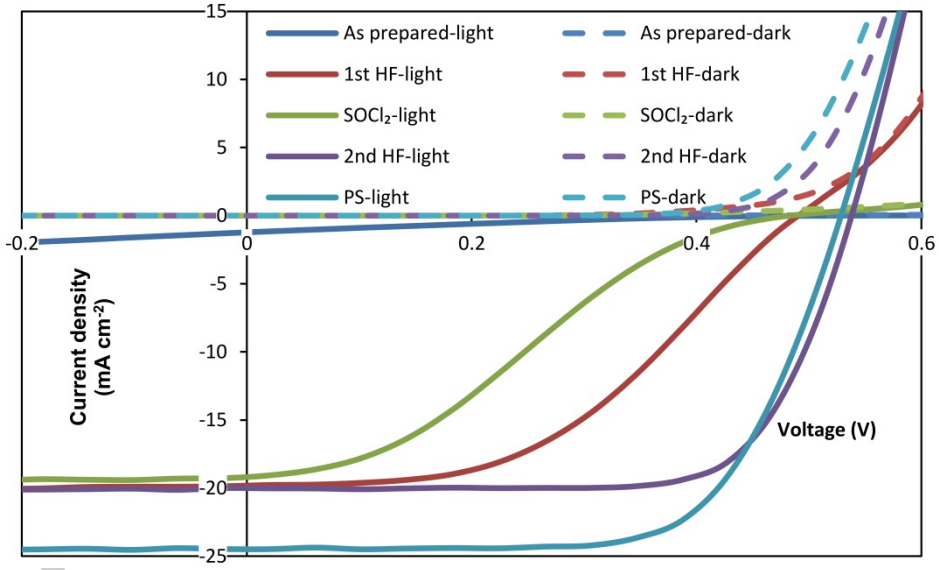

Figure 5. Light and dark current density -voltage measurements (solid lines: light curves; dashed lines: dark curves) of device with 4-layer structure Si-PEDOT:PSS-CNT-PS (after all post treatments (HF-SOCl2-HF) and adding PS antireflection layer).

Si-PANI-CNT decreases from 0.43 to 0.39 V from the first to third day, as shown in Table 3, could possibly indicate a change in the electronic nature of the heterojunction; a deprotonation process would cause a change in the Fermi level of the polymer and also lead to a less conducting interlayer. For the other three kinds of cells (Si-CNT, Si-P3HT-CNT and Si-PEDOT:PSS-CNT), the change of V_{oc} is likely caused by the growth of the silicon oxide layer.

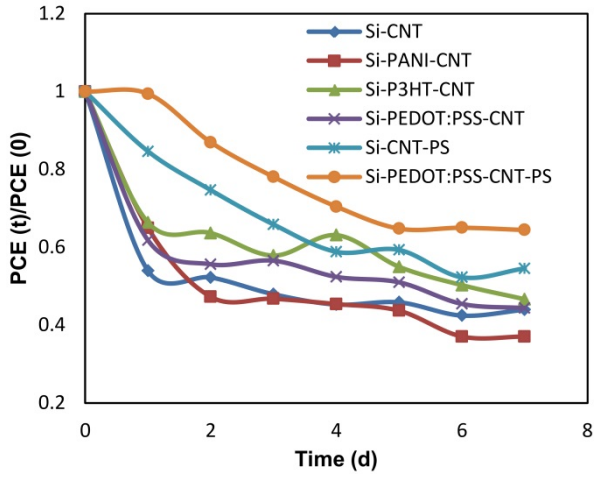

Figure 6. Degradation (of PCE) comparison among Si-CNT, Si-PANI-CNT, Si-P3HT-CNT, Si-PEDOT:PSS-CNT, Si-CNT-PS and Si-PEDOT:PSS-CNT-PS devices over 1 week; PCE (t) represents the efficiency after t days and PCE (t)/PCE (0) is the relative change in efficiency compared to the original. The degradation details of Si-CNT, Si-PANI-CNT, Si-P3HT-CNT and Si-PEDOT:PSS-CNT have been shown in Figure S5.

Table 3. Degradation of V_{oc} comparison among Si-CNT, Si-PANI-CNT, Si-P3HT-CNT and Si-PEDOT:PSS-CNT devices at 0, 1, 3, 5, and 7 days.

Cell architecture	V_{oc} (V) of cell after *x* days				
	0 d	1 d	3 d	5 d	7 d
Si-CNT	0.51	0.43	0.43	0.43	0.44
Si-PANI-CNT	0.54	0.43	0.39	0.39	0.39
Si-P3HT-CNT	0.43	0.40	0.42	0.42	0.43
S-PEDOT:PSS-CNT	0.52	0.44	0.43	0.42	0.43

Clearly, the Si-CNT-PS device has a slower decay rate than that of Si-CNT and Si-CP-CNT devices, with the performance stabilizing after 4 days (shown in detail in Figure S6, and Table S1). This is probably because PS creates a seal above the working area which prevents oxidation of the silicon surface. In contrast, the conducting polymer layers are thin, rough and unlikely to create a seal capable of protecting the silicon surface from oxidation. This could partially explain the faster degradation of conducting polymer coated devices compared to the PS coated device. The Si-PEDOT:PSS-CNT-PS sample has the slowest degradation rate of all devices studied. In this case, PS not only protects oxygen from reacting with silicon but also limits the interaction of the residual PSS with atmospheric water which reduces the conductivity of PEDOT:PSS layer. After 5 days, the performance of the device tends to be stable at a PCE of about 5.5 %.

Compared to the typical Si-CNT solar cells, the implementation of different types of polymers as interlayers is a fairly novel and an interesting topic because of the relatively straightforward fabrication approaches and the potentially lower price of the materials. The simplicity and scalability of the implementation of such an approach has several advantages. Polymers can usually be dissolved in a variety of solvents which means flexibility to meet a variety of fabrication conditions to deal with temperature requirements or perhaps application to various substrates. Polymers also afford a level of chemical control which can be very useful in processing. Uniform polymer films can be formed by using some simple, well established technology, and baking of the polymer on a surface always can be achieved at relatively low temperatures (less than 200 °C). In terms of the price of polymers, some polymer materials such as PS are already manufactured easily on a large scale. Although some other polymers are still difficult to synthesize at low cost, including these relatively novel conducting polymers-PANI, P3HT and PEDOT:PSS, the prices have decreased dramatically since the discovery of these materials. However, there are still some challenges and the limited lifespan of the resulting device will need to be further improved. In terms of future work, using CNT-polymer composites as the electrode to achieve better contact between CNT and silicon is very attractive. Using different types of CNTs such as double-walled carbon nanotubes which have been shown to have better charge carrying capability than single-walled carbon nanotubes, it may be possible to attain even better solar cell performance [13]. Therefore, although there are still quite a few barriers between current research and the realization of a commercial device, the future of this new generation of solar device with polymer interlayers is promising.

Conclusions

By building three types of solar cells with different structures (silicon-carbon nanotube, silicon-conducting polymer, and silicon-conducting polymer-carbon nanotube) and by studying three selected conducting polymers (PANI, P3HT and PEDOT:PSS), we find that conducting polymer interlayers are able to reproducibly improve the performance of Si-CNT solar cells significantly. This is likely due to the formation of a better depletion region in the silicon, resulting in increases of J_{sc}, V_{oc}, FF and PCE. The devices with PEDOT:PSS interlayers had FFs of up to 0.72 and J_{sc} of up to 20 mA cm^{-2}, yielding PCEs of up to 7.7 %. By further adding a PS antireflection top layer, J_{sc} was increased to 24.5 mA cm^{-2}, yielding a PCE of 8.7 %, with the added benefit of also protecting the silicon surface from oxidation, leading to an improvement in device stability.

Experimental Section

Polymer layers were deposited from dilute solutions of commercial polymer materials. For PANI, an emeraldine salt solution was prepared by dissolving emeraldine base (M_w: 10 000, Sigma-Aldrich, Australia) in acetic acid (80 % v/v) at a concentration of 0.58 mg mL^{-1}. The P3HT solution was prepared by dissolving P3HT solid (M_w: 63 000, Sigma-Aldrich, Australia) in toluene at a concentration of 0.45 mg mL^{-1}. PEDOT:PSS suspension was diluted 10 times from stock (Clevios PVPAI 4083) and its concentration was 1.5 mg mL^{-1}. All conducting polymer solutions were passed through Teflon filters (0.45 µm) to remove large particles in order to reduce defects during film formation. PS solutions were prepared by dissolving PS (M_w: 230 000, Sigma-Aldrich, Australia) in toluene at 2.2 wt%.

Arc-discharged CNT powder (5 mg, P3-SWNT, Carbon Solutions Inc., USA) was bath sonicated in TritonX-100 (50 mL, 1 % v/v, Sigma-Aldrich, Australia) aqueous solution at room temperature for 1 h. The CNT suspension was centrifuged at 17 500 g for 1 h. Then, the bottom residue was discarded and the supernatant was then centrifuged in the same manner as the previous one. The second supernatant of CNT/TritonX-100 was collected and then used in the following procedures as the stock suspension.

In order to balance the better conductivity and high optical transmittance of the CNT film, a dilution of 460 µL cm^{-2} CNT suspension in aqueous TritonX-100 (0.01 % v/v 250 mL) was filtered to produce 70 % transmittance CNT films. By vacuum filtration, the diluted CNT suspension was collected onto a 'target' mixed cellulose ester (MCE) membrane (0.45 µm, HAWP, Millipore, Australia) under the help of a nitrocellulose 'stencil' membrane (25 nm, VSWP, Millipore, Australia) with 4 X 0.49 cm^2 holes. The flow rate of suspension through the different pore sizes in the 'target' and 'stencil' membrane leads to a faster flow rate in region of the four holes and hence four of the identical CNT membranes can be collected on a single MCE membrane in one filtration. After filtration of the suspension, the films were rinsed sequentially by 3 X 50 mL water followed by a further 250 mL of water to remove the TritonX-100 completely. A smaller circular area (0.32 cm^2) was cut out from the MCE for device fabrication.

n-type silicon wafer doped by phosphorous (5-10 Ω cm, 525 µm thick with a 100 nm thermal oxide, ABC GmbH, Germany) were used as the substrate for device fabrication. Positive photoresist (AZ1518, micro resist technology GmbH, Munich, Germany) was spin-coated onto silicon wafer (3000 rpm, 30 s) and then soft-baked for 1 min at 100 °C. After cooling, a mask was put on top of photoresist and an active area (0.079 cm^2) was defined under the exposure of UV light for 3 min. The photoresist was developed by immersing in basic developer solution (AZ 326 MIF, AZ electronic Materials, GmbH, Munich, Germany) for 1 min and dried under a stream of nitrogen. A Ti/Au (5/145 nm) front electrode was applied using a sputter coater (with quartz crystal microbalance to control the thickness, Quorumtech K757X). Then, the substrate was immersed in acetone for 30 min followed by mild sonication (90 s) in order to dissolve the photoresist. One drop of buffer oxide etch (BOE, 6:1 of 40% NH_4F and 49% hydrofluoric acid (HF), Sigma-Aldrich, Australia) was used to remove the 100 nm thick front thermal oxide layer. At this point either (a) a CNT film was applied to prepare Si-CNT devices or (b) a conducting polymer film was used to prepare Si-CP and Si-CP-CNT devices.

To prepare Si-CNT devices and to deposit CNT film onto Si-CP devices, the circular CNT/MCE films were placed on top of substrates (CNT side down). A droplet of water was applied to wet the film and the device was baked at 80 °C in an oven for 15 min. After cooling overnight at room temperature, the acetone wash (3 X 30 min) was used to dissolve the MCE. Following scratching the rear oxide layer of silicon substrates, a gallium indium eutectic (eGaIn) was used to mount the cells onto stainless steel plates. These are referred to as the 'as-prepared' devices (Figure 1). To measure the transmittance and the sheet resistance, CNT/MCE films were transferred onto a glass slide in the same manner and the same process was used to dissolve the MCE.

To prepare Si-CP devices, all polymers were spin-coated (3000 rpm, 3 drops during 30 s) onto silicon substrates after etching the thermal oxide layer. PANI devices were baked at 130 °C for 2 h [12a]. Different amounts of PANI solution (0, 3, 5, 10 and 15 drops) were spin-coated on silicon at 3000 rpm to vary the layer thickness. P3HT devices were baked at 130 °C for 20 min [14]. A drop of methanol was put on the active area of PEDOT:PSS devices which were then baked at 130 °C for 20 min [15]. Following cooling, the substrates with PEDOT:PSS were dipped into methanol for 10 min and dried at 140 °C for 5 min. This is used to improve the stability of PEDOT:PSS film when exposed to ambient conditions [15-16]. Each of these conducting polymer devices were completed in triplicate and all heating steps were conducted using a hot plate. For those devices without CNT films, etching of the rear oxide layer and assembly of cells were conducted after applying the polymer layer. The PS antireflection layer was spin-coated (6500 rpm, 90 s) to the cells after all post treatments described in the next section.

There are 3 post treatments for the as-prepared devices. Firstly, the active area was covered with HF (2%) for 10 s before rinsing with water, ethanol and drying with nitrogen to etch the oxide layer formed during the cell fabrication. Since HF can react with glass and ruin the sample, HCl was used for the acid treatment on the CNT/glass surface to detect the transmittance and sheet resistance. The $SOCl_2$ treatment was done by placing 2 drops onto the CNT film on silicon substrate or glass slides and after the doping process, the surface was rinsed with ethanol and blown dry with nitrogen. This step is used to improve the conductivity of the film by electron transfer from the valence band of CNT to the strong organic oxidizer [3d]. The second HF treatment was accomplished in the same way as the first one to remove the oxide layer formed during the $SOCl_2$ treatment and this revealed the influence the $SOCl_2$ on the performance of the devices.

Transmittance of CNT films was evaluated by averaging the absorption values from 2 wavelengths (450 and 850 nm) in UV-Vis-NIR spectra. Reflectance spectra were measured from 350 to 1500 nm by Perkin Elmer UV-Vis-NIR Lambda 950. CNT film (r = 9 mm) was applied on a silicon wafer and PS (2.2 wt% in toluene) layer was then spin-coated on it at 6500 rpm for 90 s. A light beam passed through the CNT films on the glass slides while a clean slide was used for background subtraction. Sheet resistance of the CNT films on glass was measured by a four point probe (Keithlink). The thickness and the morphology the polymer layers were determined by atomic force microscope (Nanoscope, Multimode, Bruker) by measuring the samples on silicon surfaces. Several scratches were made by a surgical scalpel for thickness determination. In order to record and analyze the current density-voltage data of the devices, a Keithley 2400 source measure unit was used with a custom Labview™ virtual instrument. A standard silicon test cell with NIST-traceable certification was used to calibrate the power density as 100 mW cm^{-2} at the sample plane of the collimated xenon-arc light source, which was passed through an AM 1.5G filter. The light and dark curves are measured to determine the performance and the diode properties of the devices. In dark curves, the diode properties were assessed by using the following equation [17].

$$J = J_{sat} (\exp((qV)/(nkT))-1)$$

J_{sat}: reverse saturation current; *q*: elemental charge; *V*: applied voltage; *n*: ideality; *k*: Boltzmann constant; *T*: temperature

For qV > nkT, -1 term can be omitted because it is very small compared to $e^{\frac{qV}{nkT}}$ term. Taking the logarithm of both sides leads to the following equation

$$\ln J = (qV)/(nkT) + \ln J_{sat}$$

By plotting ln J versus V, the n and the J_{sat} can be calculated from the slope and the y-intercept.

Acknowledgements

This work is supported by the Australian Microscopy and Microanalysis Research Facility (AMMRF). Thanks to Professor David Lewis (Flinders University, South Australia) for providing polymer materials (PS, PANI, P3HT and PEDOT:PSS).

Keywords: carbon nanotubes • conducting polymers • solar cells

[1] D. D. Tune, B. S. Flavel, R. Krupke, J. G. Shapter, *Adv. Energy Mater.* **2012**, *2*, 1043-1055.

[2] a) C. T. White, T. N. Todorov, *Nature* **1998**, *393*, 240-242; b) J. Maultzsch, R. Pomraenke, S. Reich, E. Chang, D. Prezzi, A. Ruini, E. Molinari, M. S. Strano, C. Thomsen, C. Lienau, *Phys. Rev. B* **2005**, *72*; c) C. D. Spataru, F. Leonard, *Phys. Rev. Lett.* **2010**, *104*; d) S. J. Wang, M. Khafizov, X. M. Tu, M. Zheng, T. D. Krauss, *Nano Lett.* **2010**, *10*, 2381-2386; e) S. Iijima, *Nature* **1991**, *354*, 56-58.

[3] a) J. Q. Wei, Y. Jia, Q. K. Shu, Z. Y. Gu, K. L. Wang, D. M. Zhuang, G. Zhang, Z. C. Wang, J. B. Luo, A. Y. Cao, D. H. Wu, *Nano Lett.* **2007**, *7*; b) A. Behnam, J. L. Johnson, Y. Choi, M. G. n. Ertosun, A. K. Okyay, P. Kapur, K. C. Saraswat, A. Ural, *Appl. Phys. Lett.* **2008**, *92*, 243116; c) Y. Jia, J. Wei, K. Wang, A. Cao, Q. Shu, X. Gui, Y. Zhu, D. Zhuang, G. Zhang, B. Ma, L. Wang, W. Liu, Z. Wang, J. Luo, D. Wu, *Adv. Mater.* **2008**, *20*, 4594-4598; d) Z. Li, V. P. Kunets, V. Saini, Y. Xu, E. Dervishi, G. J. Salamo, A. R. Biris, A. S. Biris, *Appl. Phys. Lett.* **2008**, *93*, 243117; e) Y. Jia, A. Y. Cao, X. Bai, Z. Li, L. H. Zhang, N. Guo, J. Q. Wei, K. L. Wang, H. W. Zhu, D. H. Wu, P. M. Ajayan, *Nano Lett.* **2011**, *11*, 1901-1905; f) Y. Jia, A. Y. Cao, F. Y. Kang, P. X. Li, X. C. Gui, L. H. Zhang, E. Z. Shi, J. Q. Wei, K. L. Wang, H. W. Zhu, D. H. Wu, *Phys. Chem. Chem. Phys.* **2012**, *14*, 8391-8396; g) Y. Jia, P. Li, X. Gui, J. Wei, K. Wang, H. Zhu, D. Wu, L. Zhang, A. Cao, Y. Xu, *Appl. Phys. Lett.* **2011**, *98*, 133115; h) Y. Jia, P. X. Li, J. Q. Wei, A. Y. Cao, K. L. Wang, C. L. Li, D. M. Zhuang, H. W. Zhu, D. H. Wu, *Mater. Res. Bull.* **2010**, *45*, 1401-1405; i) P. Wadhwa, B. Liu, M. A. McCarthy, Z. C. Wu, A. G. Rinzler, *Nano Lett.* **2010**, *10*, 5001-5005; j) D. D. Tune, F. Hennrich, S. Dehm, M. F. G. Klein, K. Glaser, A. Colsmann, J. G. Shapter, U. Lemmer, M. M. Kappes, R. Krupke, B. S. Flavel, *Adv. Energy Mater.* **2013**, *3*, 1091-1097; k) D. D. Tune, A. J. Blanch, R. Krupke, B. S. Flavel, J. G. Shapter, *Phys. Status Solidi A* **2014**, *211*, 1479-1487; l) D. D. Tune, J. G. Shapter, *Nanomaterials* **2013**, *3*, 655-673.

[4] a) S. Gunes, H. Neugebauer, N. S. Sariciftci, *Chem. Rev.* **2007**, *107*, 1324-1338; b) M. Jorgensen, K. Norrman, F. C. Krebs, *Sol. Energy Mater. Sol. Cells* **2008**, *92*, 686-714; c) B. C. Thompson, J. M. J. Frechet, *Angew. Chem. Int. Ed.* **2008**, *47*, 58-77; d) L. M. Chen, Z. R. Hong, G. Li, Y. Yang, *Adv. Mater.* **2009**, *21*, 1434-1449; e) G. Dennler, M. C. Scharber, C. J. Brabec, *Adv. Mater.* **2009**, *21*, 1323-1338; f) F. C. Krebs, *Sol. Energy Mater. Sol. Cells* **2009**, *93*, 394-412; g) G. Li, R. Zhu, Y. Yang, *Nat. Photonics* **2012**, *6*, 153-161.

[5] a) J. Zhang, T. Song, X. Shen, X. Yu, S. T. Lee, B. Sun, *ACS Nano* **2014**, *8*, 11369-11369; b) R. Liu, S. T. Lee, B. Sun, *Adv Mater* **2014**, *26*, 6007-6012; c) X. J. Shen, B. Q. Sun, D. Liu, S. T. Lee, *Journal of the American Chemical Society* **2011**, *133*, 19408-19415; d) Y. F. Zhang, F. S. Zu, S. T. Lee, L. S. Liao, N. Zhao, B. Q. Sun, *Adv. Energy Mater.* **2014**, *4*; e) Y. Zhang, W. Cui, Y. Zhu, F. Zu, L. Liao, S.-T. Lee, B. Sun, *Energy Environ. Sci.* **2015**.

[6] E. Z. Shi, L. H. Zhang, Z. Li, P. X. Li, Y. Y. Shang, Y. Jia, J. Q. Wei, K. L. Wang, H. W. Zhu, D. H. Wu, S. Zhang, A. Y. Cao, *Sci Rep* **2012**, *2*, 5.

[7] J. B. You, L. T. Dou, K. Yoshimura, T. Kato, K. Ohya, T. Moriarty, K. Emery, C. C. Chen, J. Gao, G. Li, Y. Yang, *Nat. Commun.* **2013**, *4*, 10.

[8] R. Li, J. Di, Z. Yong, B. Sun, Q. Li, *J. Mater. Chem.* **2014**, *2*, 4140.

[9] W. N. Wang, E. A. Schiff, *Appl. Phys. Lett.* **2007**, *91*, 3.

[10] a) L. N. He, C. Y. Jiang, H. Wang, H. Lei, D. Lai, Rusli, Ieee, *2012 38th Ieee Photovoltaic Specialists Conference (Pvsc)* **2012**, 2785-2787; b) B. Ozdemir, M. Kulakci, R. Turan, H. E. Unalan, *Appl. Phys. Lett.* **2011**, *99*, 3; c) S. C. Shiu, J. J. Chao, S. C. Hung, C. L. Yeh, C. F. Lin, *Chem. Mater.* **2010**, *22*, 3108-3113.

[11] K. A. Nagamatsu, S. Avasthi, J. Jhaveri, J. C. Sturm, *Ieee Journal of Photovoltaics* **2014**, *4*, 260-264.

[12] a) D. D. Tune, B. S. Flavel, J. S. Quinton, A. V. Ellis, J. G. Shapter, *ChemSusChem* **2013**, *6*, 320-327; b) S. E. Bourdo, V. Saini, J. Piron, I. Al-Brahim, C. Boyer, J. Rioux, V. Bairi, A. S. Biris, T. Viswanathan, *ACS Appl. Mater. Interfaces* **2012**, *4*, 363-368.

[13] K. E. Moore, B. S. Flavel, C. J. Shearer, A. V. Ellis, J. G. Shapter, *Electrochemistry Communications* **2011**, *13*, 1190-1193.

[14] S. Van Bavel, E. Sourty, G. De With, K. Frolic, J. Loos, *Macromolecules* **2009**, *42*, 7396-7403.

[15] D. Alemu, H.-Y. Wei, K.-C. Ho, C.-W. Chu, *Energy Environ. Sci.* **2012**, *5*, 9662.

[16] a) J. S. Huang, P. F. Miller, J. S. Wilson, A. J. de Mello, J. C. de Mello, D. D. C. Bradley, *Adv. Funct. Mater.* **2005**, *15*, 290-296; b) A. M. Nardes, M. Kemerink, M. M. de Kok, E. Vinken, K. Maturova, R. A. J. Janssen, *Org. Electron.* **2008**, *9*, 727-734; c) A. Denneulin, A. Blayo, J. Bras, C. Neuman, *Prog. Org. Coat.* **2008**, *63*, 87-91.

[17] S. K. Cheung, N. W. Cheung, *Appl. Phys. Lett.* **1986**, *49*, 85-87.

FULL PAPER

Carbon nanotube-silicon heterojunction solar cells have been studied in recent years. Application of a conducting polymer interlayer between the silicon surface and carbon nanotube film can improve the performance of the devices. This provides a simple and potentially economic approach to achieve a higher efficiency device.

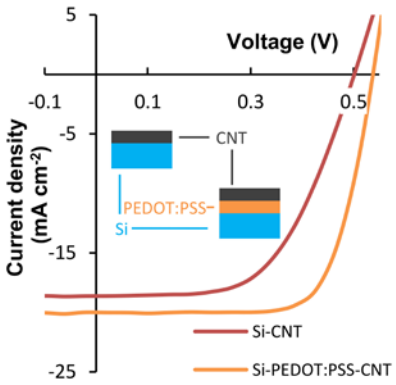

*Leping Yu, Daniel D. Tune, Cameron J. Shearer and Joseph G. Shapter**

Page No. – Page No.

Application of Polymer Interlayers in Silicon-Carbon Nanotube Heterojunction Solar Cells